

# *Pyropia yezoensis* protein protects against TNF- $\alpha$ -induced myotube atrophy in C2C12 myotubes via the NF- $\kappa$ B signaling pathway

MIN-KYEONG LEE<sup>1</sup>, YOUN HEE CHOI<sup>1,2</sup> and TAEK-JEONG NAM<sup>1</sup>

<sup>1</sup>Institute of Fisheries Sciences, Pukyong National University, Busan 46041;

<sup>2</sup>Department of Marine Bio-Materials & Aquaculture, Pukyong National University, Busan 48513, Republic of Korea

Received September 15, 2020; Accepted April 12, 2021

DOI: 10.3892/mmr.2021.12125

**Abstract.** The protein extracted from red algae *Pyropia yezoensis* has various biological activities, including anti-inflammatory, anticancer, antioxidant, and antiobesity properties. However, the effects of *P. yezoensis* protein (PYCP) on tumor necrosis factor- $\alpha$  (TNF- $\alpha$ )-induced muscle atrophy are unknown. Therefore, the present study investigated the protective effects and related mechanisms of PYCP against TNF- $\alpha$ -induced myotube atrophy in C2C12 myotubes. Treatment with TNF- $\alpha$  (20 ng/ml) for 48 h significantly reduced myotube viability and diameter and increased intracellular reactive oxygen species levels; these effects were significantly reversed in a dose-dependent manner following treatment with 25-100  $\mu$ g/ml PYCP. PYCP inhibited the expression of TNF receptor-1 in TNF- $\alpha$ -induced myotubes. In addition, PYCP markedly downregulated the nuclear translocation of nuclear factor- $\kappa$ B (NF- $\kappa$ B) by inhibiting the phosphorylation of inhibitor of  $\kappa$ B. Furthermore, PYCP treatment suppressed 20S proteasome activity, IL-6 production, and the expression of the E3 ubiquitin ligases, atrogin-1/muscle atrophy F-box and muscle RING-finger protein-1. Finally, PYCP treatment increased the protein expression levels of myoblast determination protein 1 and myogenin in TNF- $\alpha$ -induced myotubes. The present findings indicate that PYCP may protect against TNF- $\alpha$ -induced myotube atrophy by inhibiting the proinflammatory NF- $\kappa$ B pathway.

## Introduction

Skeletal muscle atrophy is caused by various chronic diseases, including obesity, cancer, diabetes, heart failure, AIDS, sepsis, and rheumatoid arthritis (1). Atrophy also occurs in aging, starvation, and muscle denervation, as well as in

genetic myopathies, such as muscular dystrophies, leading to a decrease in muscle strength and mass (2). Muscle atrophy is caused by decreased protein synthesis and increased proteolysis, due primarily to hyperactivation of major cellular degradation pathways, including the ubiquitin-proteasome and autophagy-lysosomal systems (3-5). Proinflammatory cytokines, such as tumor necrosis factor- $\alpha$  (TNF- $\alpha$ ), interleukin (IL)-1 $\beta$ , and IL-6, have been shown to promote the breakdown of myofibrillar proteins and reduce protein synthesis, leading directly to muscle loss (3-5). Among the cytokines, TNF- $\alpha$  induces ubiquitin-dependent proteolysis by activating various intracellular factors, including reactive oxygen species (ROS), nuclear factor- $\kappa$ B (NF- $\kappa$ B), atrogin-1/muscle atrophy F-box (MAFbx), and muscle RING-finger protein-1 (MuRF1), as well as apoptosis (3-5).

TNF- $\alpha$ , a proinflammatory cytokine, has been implicated in muscle catabolic conditions and has an important role in a variety of biological processes, including cell growth and differentiation (6), inflammation (7), apoptosis, and necrosis (8). Among its various effects on skeletal muscle protein, TNF- $\alpha$  induces anabolic and catabolic effects regulated by different signaling pathways. TNF- $\alpha$  acts by binding to TNF receptor-1 (TNF-R1) and TNF-R2 and acts as a potent activator of the NF- $\kappa$ B pathway by promoting endogenous production of ROS via mitochondrial electron transport in various cell types, including muscle (9). Phosphorylation and proteasomal degradation of the NF- $\kappa$ B inhibitory protein, inhibitor of  $\kappa$ B (I $\kappa$ B), lead to the activation and nuclear translocation of NF- $\kappa$ B (10). Activated NF- $\kappa$ B causes skeletal muscle atrophy through three potential mechanisms. First, NF- $\kappa$ B can increase the protein expression of components of the ubiquitin-proteasome system, which is involved in the degradation of specific muscle proteins during muscle atrophy (11,12). Second, NF- $\kappa$ B can increase the expression of inflammation-related molecules, such as IL-1 $\beta$  and IL-6, which directly or indirectly activate muscle wasting (13). Finally, NF- $\kappa$ B can inhibit the expression of muscle differentiation-related genes, such as myoblast determination protein 1 (MyoD) and myogenin, which are involved in the regeneration of atrophied skeletal muscle (14,15). MyoD and myogenin are myogenic transcription factors that have an important role in regulating muscle differentiation, and activation of NF- $\kappa$ B is known to reduce the cellular MyoD and myogenin protein levels through post-transcriptional

---

*Correspondence to:* Professor Taek-Jeong Nam, Institute of Fisheries Sciences, Pukyong National University, 474 Ilgwang-ro, Ilgwang-myeon, Gijang-gun, Busan 46041, Republic of Korea  
E-mail: namtj@pknu.ac.kr

**Key words:** tumor necrosis factor- $\alpha$ , aging, sarcopenia, myotube atrophy, *Pyropia yezoensis* protein

mechanisms (16). In summary, NF- $\kappa$ B appears to increase the ubiquitin-proteasome pathway activity, increase IL-6 expression, and inhibit myogenesis, promoting muscle protein breakdown, and leading to muscle atrophy.

Panduratin A has been shown to increase the TNF- $\alpha$ -induced decrease in MyoD and myogenin mRNA expression and attenuate the TNF- $\alpha$ -induced increase in atrogin-1/MAFbx and MAFbx mRNA expression, and significantly inhibit the production of ROS by increasing the mRNA expression of catalase and superoxide dismutase in L6 myotubes (5). Furthermore, S-allyl cysteine inhibits TNF- $\alpha$ -induced muscle atrophy by suppressing endogenous pro-inflammatory molecules TNF- $\alpha$ , IL-6, TNF-like weak inducer of apoptosis (TWEAK), TWEAK receptor fibroblast growth factor-inducible receptor 14, IL-1 $\beta$ , NF- $\kappa$ B, and E3 ubiquitin ligases, and inhibiting the degradation of muscle-specific structural protein, fast myosin heavy chain (MHCf) (7). Therefore, regulating both TNF- $\alpha$ -induced oxidative stress and the NF- $\kappa$ B pathway is an important strategy for improving muscle disorders, such as muscle atrophy.

*Pyropia yezoensis* is a commercially important edible red alga in Southeast Asia, including Korea, China, Japan, and Taiwan (17). *P. yezoensis* contains biologically active phytochemicals, such as proteins, polysaccharides, essential fatty acids, vitamins, minerals, tocopherols, carotenoids, and phycocyanins (17). In particular, its high protein content (25-50%, dry matter basis) serves as a source of bioactive peptides with antimuscular atrophy (18), antioxidant (19), anticancer (20), anti-inflammatory (21), collagen synthesis (22), and hepatoprotective effects (23). A previous study on the muscle atrophy protection mechanism of *P. yezoensis* protein (PYCP) showed that PYCP prevented dexamethasone-induced muscle atrophy in mice by increasing protein synthesis and decreasing protein degradation via inhibiting the ubiquitin-proteasome and autophagy-lysosomal pathways (18). However, the efficacy of PYCP in the prevention of muscle atrophy due to chronic low-grade inflammation has not yet been demonstrated. Therefore, the present study investigated the protective mechanisms and therapeutic potential of PYCP on TNF- $\alpha$ -induced myotube atrophy in C2C12 myotubes.

## Materials and methods

**Preparation of PYCP.** *P. yezoensis* was purchased from Suhyup, the National Federation of Fisheries Cooperatives (Busan, Korea), washed several times with tap water to remove salt and visible epiphytes and stored at -50°C until use. *P. yezoensis* powder (8 g) was diluted with 300 ml Tris-HCl buffer (50 mM, pH 7.8) and stirred at 4°C for 1 h. The solution was centrifuged at 3,134 x g at 4°C for 20 min and vacuum-filtered through a crucible. The supernatant was added to 80% (NH<sub>4</sub>)<sub>2</sub>SO<sub>4</sub> and stirred at 4°C for 24 h, then centrifuged at 173,502 x g at 4°C for 30 min. After dissolving the precipitate in Tris-HCl buffer, the salt was removed by dialysis at 4°C for 72 h using a Spectra/Por membrane (Spectrum Laboratories, Ltd.) with a molecular weight cutoff of 3.5 kDa. The dialyzed solution was distributed into 1.5-ml tubes and freeze-dried. The lyophilized powder (termed PYCP) was stored at -70°C until use. PYCP was solubilized in phosphate-buffered saline (PBS) for use in assays.

**C2C12 cell culture and differentiation.** Myoblasts derived from mouse skeletal muscle (cat. no. CRL-1772; American Type Culture Collection) were cultured in 6-well plates containing Dulbecco's modified Eagle's medium (DMEM; Gibco; Thermo Fisher Scientific, Inc.) supplemented with 10% fetal bovine serum (FBS; Gibco; Thermo Fisher Scientific, Inc.), 100 U/ml penicillin, and 100  $\mu$ g/ml streptomycin (Gibco; Thermo Fisher Scientific, Inc.) at 37°C in a humidified atmosphere of 5% CO<sub>2</sub>. When myoblasts were approximately 80-90% confluent, myotube differentiation was initiated by replacing the growth medium with differentiation medium: DMEM supplemented with 2% FBS. Differentiation was allowed to proceed for 6 days, with the medium changed every 48 h, at which stage 90-100% of the cells had fused into myotubes.

**Treatment of cells with recombinant TNF- $\alpha$  and PYCP.** TNF- $\alpha$  (PeproTech, Inc.) was dissolved in PBS to a final concentration of 10  $\mu$ g/ml for the stock solution and then diluted to the indicated concentrations. Differentiated myotubes were treated with 20 ng/ml TNF- $\alpha$ , various concentrations of PYCP (25, 50 or 100  $\mu$ g/ml), or both factors in combination for 48 h. For the control group, the myotubes were incubated with differentiation medium and PBS only.

**Cell viability assay.** Cell viability was determined using the CellTiter 96 Aqueous Cell Proliferation Assay (Promega Corporation), which is based on the formation of a formazan product from the tetrazolium compound (3-(4,5-dimethylthiazol-2-yl)-5-(3-carboxymethoxyphenyl)-2-(4-sulfonyl)-2H-tetrazolium (MTS). Cells (1.5x10<sup>4</sup> cells/well) were seeded into 96-well plates in 100  $\mu$ l DMEM supplemented with 10% FBS and were allowed to attach at 37°C for 24 h. Following differentiation as aforementioned, the cells were incubated with 20 ng/ml TNF- $\alpha$  and PYCP (25, 50, or 100  $\mu$ g/ml) at 37°C for 48 h. MTS solution (10  $\mu$ l) was added, and the cells were incubated at 37°C for 30 min. The absorbance at 490 nm was measured using a Gen5 microplate reader (BioTek Instruments, Inc.). Experiments were performed in triplicate.

**Measurement of myotube diameter.** Myotube cultures were photographed under a phase-contrast microscope at x20 magnification following treatment with 20 ng/ml TNF- $\alpha$  and 25, 50, or 100  $\mu$ g/ml PYCP for 48 h. Myotube diameters were determined based on the method described by Castillero *et al* and Menconi *et al* (24,25). The average diameter of each myotube was calculated as the mean of five different myotube measurements in 10 different fields (n=50) using ImageJ software (version 4.16; National Institutes of Health). The measurements were conducted by a researcher blinded to the origin of the experimental groups.

**Measurement of intracellular ROS production.** Intracellular ROS were detected using the redox-sensitive fluorescent dye 2'-7'-dichlorofluorescein diacetate [DCF-DA (C<sub>24</sub>H<sub>14</sub>C<sub>12</sub>O<sub>7</sub>); Sigma-Aldrich; Merck KGaA). Cells were plated at 1.5x10<sup>4</sup> cells/well in 96-well plates overnight and differentiated into myotubes for 6 days. Following differentiation, the cells were incubated with 20 ng/ml TNF- $\alpha$  and PYCP (25, 50, or 100  $\mu$ g/ml) at 37°C for 48 h. At the end of the treatment,

cells were washed with cold PBS and incubated with 20  $\mu$ M DCF-DA at 37°C for 30 min. Following incubation, the cells were washed with cold PBS. Fluorescence intensities of the stained cells were determined at excitation and emission wavelengths of 485 and 535 nm, respectively, using a Gen5 microplate fluorescence reader (BioTek Instruments, Inc.).

**Measurement of IL-6 production.** IL-6 was measured in the supernatant using an ELISA kit (cat. no. M6000B; R&D Systems, Inc.), according to the manufacturer's instructions. Briefly, a monoclonal antibody specific for mouse IL-6 was coated onto the microplates. After adding 50  $\mu$ l of standard or sample, 50  $\mu$ l of assay diluent (RD1-14) was added to the center of each well. Wells were incubated at room temperature for 2 h, then washed five times. Afterward, 100  $\mu$ l of mouse IL-6 conjugate was added to each well, and the plate was incubated for another 2 h, followed by repeated washing. Lastly, wells were incubated in 100  $\mu$ l of substrate solution for 30 min and stopped with stop solution. The optical density of each well was determined at 450 nm and corrected at 570 nm.

**Measurement of 20S proteasome activity.** The chymotrypsin-like activity of the 20S proteasome was measured based on changes in the fluorescence of 7-amino-4-methylcoumarin (AMC) conjugated to the chymotrypsin peptide substrate LLVY using a 20S proteasome activity kit (Chemicon; Thermo Fisher Scientific, Inc.). In brief, cells were suspended in RIPA lysis buffer (50 mM Tris-HCl, pH 7.5, 150 mM NaCl, 0.5% sodium deoxycholate, 1% Triton X-100, 0.1% SDS, and 2 mM EDTA) containing protease inhibitors (1 mg/ml aprotinin, 1 mg/ml leupeptin, 1 mg/ml pepstatin A, 200 mM Na<sub>3</sub>VO<sub>4</sub>, 500 mM NaF, and 100 mM PMSF) and centrifuged at 16,000 x g at 4°C for 10 min. The protein concentration of supernatants was determined with a bicinchoninic acid (BCA) protein assay (Pierce; Thermo Fisher Scientific, Inc.). The cell lysates were incubated with a labeled substrate, LLVY-AMC, at 37°C for 90 min. The cleavage activity was monitored by detecting the free fluorophore AMC using a Gen5 microplate reader (BioTek Instruments, Inc.) (18).

**Preparation of total cell lysate.** After C2C12 myoblasts were differentiated for 6 days, myotubes were treated with 20 ng/ml TNF- $\alpha$  and PYCP (25, 50, or 100  $\mu$ g/ml) at 37°C for 48 h. Cells were washed twice with PBS (Gibco; Thermo Fisher Scientific, Inc.) and lysed with extraction buffer [1% NP-40, 0.25% sodium deoxycholate, 1 mM ethylene glycol-bis( $\beta$ -aminoethyl ether)-N,N,N',N'-tetra-acetic acid, 150 mM NaCl, and 50 mM Tris-HCl, pH 7.5] containing protease inhibitors (1 mg/ml aprotinin, 1 mg/ml leupeptin, 1 mg/ml pepstatin A, 200 mM Na<sub>3</sub>VO<sub>4</sub>, 500 mM NaF, and 100 mM PMSF) on ice. After incubation at 4°C for 30 min, the extracts were centrifuged at 16,000 x g at 4°C for 10 min. The protein levels in the supernatants were quantified using a BCA protein assay kit (Pierce; Thermo Fisher Scientific, Inc.), according to the manufacturer's instructions. The supernatant was then used in western blot analysis (18).

**Preparation of cytosolic and nuclear extracts.** Cells were treated and harvested as described for the total cell lysate extraction. Cells were then lysed with hypotonic lysis buffer

(25 mM HEPES pH 7.5, 5 mM EDTA, 5 mM MgCl<sub>2</sub>, and 5 mM DTT) containing protease inhibitors (1 mg/ml aprotinin, 1 mg/ml leupeptin, 1 mg/ml pepstatin A, 200 mM Na<sub>3</sub>VO<sub>4</sub>, 500 mM NaF, and 100 mM PMSF), and incubated on ice for 10 min. Cells were further lysed by adding ice-cold NP-40 to a final concentration of 2.5%. The tubes were vortexed on the highest setting for 5 sec. After incubation on ice for another 10 min, the tubes were vortexed again on the highest setting for 5 sec, then centrifuged at 16,000 x g at 4°C for 5 min. The supernatant (cytoplasmic extract) was immediately transferred to clean, pre-chilled tubes. The insoluble (pellet) fraction containing nuclei was resuspended in ice-cold cell extraction buffer (10 mM HEPES pH 7.9, 100 mM NaCl, 1.5 mM MgCl<sub>2</sub>, 0.1 mM EDTA, and 0.2 mM DTT) containing protease inhibitor. The samples were placed on ice and vortexed for 15 sec every 10 min for a total of 40 min. The tubes were centrifuged at 16,000 x g at 4°C for 10 min. The supernatant (nuclear extract) was immediately transferred to clean, pre-chilled tubes. Protein levels were determined using a BCA protein assay kit (Pierce; Thermo Fisher Scientific, Inc.), according to the manufacturer's instructions. Both extracts were then used in western blot analysis (18).

**Western blot analysis.** Equal amounts of protein (30  $\mu$ g) were separated using 7-12.5% sodium dodecyl sulfate-polyacrylamide gel electrophoresis and transferred to polyvinylidene fluoride membranes (EMD Millipore). The membranes were blocked by incubation with 1% bovine serum albumin (BSA) in TBS-T (10 mM Tris-HCl, 150 mM NaCl, and 0.1% Tween-20) at room temperature for 90 min, and then incubated with specific primary antibodies at room temperature for 3 h (Table I). The membranes were washed three times with TBS-T and incubated for 90 min at room temperature with the appropriate horseradish peroxidase-conjugated secondary anti-rabbit IgG (cat. no. 7074S; Cell Signaling Technology, Inc.), anti-mouse IgG (cat. no. 7076S; Cell Signaling Technology, Inc.), or donkey anti-goat IgG antibodies (cat. no. A50-101P; Bethyl Laboratories, Inc.), diluted at 1:10,000-1:20,000 in TBS-T containing 1% BSA. Signals were detected using an enhanced chemiluminescence western blot analysis kit (Thermo Fisher Scientific, Inc.). Experiments were performed in triplicate, and densitometry analysis was performed using Multi-Gauge software version 3.0 (Fujifilm Life Sciences). GAPDH,  $\beta$ -actin, or lamin B1 were used as internal controls for equal protein loading in total cell, cytoplasmic or nuclear extracts, respectively (18).

**Statistical analysis.** The results are presented as the mean  $\pm$  standard deviation of at least three independent experiments. Data were analyzed by one-way analysis of variance followed by the Duncan multiple-range test using SPSS software version 18.0 (SPSS, Inc.). P<0.05 was considered to indicate a statistically significant difference.

## Results

**Effects of PYCP on cell viability.** To examine the cytotoxic effects of PYCP on mouse skeletal muscle cells, cell viability was measured using the MTS assay. C2C12 myotubes were incubated without or with PYCP at various concentrations

Table I. List of primary antibodies used in western blot analysis.

Antibody	Catalog number	Species of origin	Dilution
Atrogin-1/MAFbx	sc-27645	Goat	1:1,000
$\beta$ -actin	sc-47778	Mouse	1:1,000
GAPDH	sc-25778	Mouse	1:1,000
I $\kappa$ B $\alpha$	sc-7218	Rabbit	1:1,000
Lamin B1	sc-377000	Mouse	1:1,000
MuRF1	sc-27642	Goat	1:1,000
MyoD	sc-377186	Mouse	1:1,000
Myogenin	sc-12732	Mouse	1:1,000
NF- $\kappa$ B p65	sc-8008	Mouse	1:500
p-I $\kappa$ B $\alpha$	sc-8404	Mouse	1:1,000
TNF-R1	sc-8436	Mouse	1:1,000

All antibodies were purchased from Santa Cruz Biotechnology, Inc. MAFbx, muscle atrophy F-box; I $\kappa$ B $\alpha$ , inhibitor of  $\kappa$ B  $\alpha$ ; MuRF1, muscle RING-finger protein-1; MyoD, myoblast determination protein 1; NF- $\kappa$ B, nuclear factor- $\kappa$ B; p-, phosphorylated; TNF-R1, TNF receptor-1.

(25-100  $\mu$ g/ml). As shown in Fig. 1A, no significant toxicity was observed in myotubes treated with PYCP for 48 h. To examine the protective effects of PYCP against TNF- $\alpha$ -induced myotube damage, mouse skeletal muscle C2C12 cells were incubated with various concentrations of PYCP (25, 50, or 100  $\mu$ g/ml). As shown in Fig. 1B, the cell viability of TNF- $\alpha$ -treated myotubes was decreased compared with non-treated myotubes. However, treatment with PYCP protected cells from the TNF- $\alpha$ -induced decrease in cell viability (Fig. 1B). Therefore, 25, 50 and 100  $\mu$ g/ml PYCP were used for further experiments.

*Effects of PYCP on myotube diameter.* To investigate whether PYCP protects against myotube atrophy in TNF- $\alpha$ -stimulated C2C12 myotubes, the myotube diameter was measured. As shown in Fig. 2, the myotube diameter in TNF- $\alpha$ -treated myotubes was decreased compared with non-treated myotubes. However, TNF- $\alpha$ -treated myotubes showed a significant increase in myotube diameter in the presence of PYCP (Fig. 2).

*Effects of PYCP on TNF- $\alpha$ -induced intracellular ROS production.* To examine whether PYCP functions as a scavenger of TNF- $\alpha$ -induced ROS production, intracellular ROS levels were measured. As shown in Fig. 3, the production of ROS in TNF- $\alpha$ -treated myotubes was significantly increased compared with non-treated myotubes. However, TNF- $\alpha$ -treated myotubes exhibited a significant decrease in ROS production in the presence of PYCP in a dose-dependent manner (Fig. 3). These results indicated that PYCP inhibited the intracellular accumulation of ROS in mouse skeletal muscle cells damaged by TNF- $\alpha$ -mediated oxidative stress.

*Effects of PYCP on TNF-R1 expression.* To determine whether PYCP treatment altered the expression levels of TNF-R1 in TNF- $\alpha$ -treated C2C12 myotubes, the TNF-R1 protein expression levels were examined by western blot analysis. As shown in Fig. 4, the TNF-R1 protein expression levels were significantly increased in TNF- $\alpha$ -treated C2C12 myotubes.

However, the TNF- $\alpha$ -induced upregulation of TNF-R1 was significantly attenuated by PYCP treatment (Fig. 4).

*Effects of PYCP on the NF- $\kappa$ B signaling pathway.* To further explore the mechanism underlying transcriptional control by PYCP, C2C12 myotubes were treated with TNF- $\alpha$  (20 ng/ml) and PYCP (25, 50, or 100  $\mu$ g/ml) for 48 h, and proteins associated with NF- $\kappa$ B/p65 subunit nuclear translocation were examined by western blot analysis. As shown in Fig. 5A, the phosphorylation of I $\kappa$ B $\alpha$ , which induces NF- $\kappa$ B/p65 activation, was inhibited by PYCP treatment in TNF- $\alpha$ -induced C2C12 myotubes. Consequently, the nuclear NF- $\kappa$ B/p65 levels were significantly decreased by PYCP treatment compared with TNF- $\alpha$ -only treated C2C12 myotubes (Fig. 5B). The results indicated that PYCP treatment effectively blocked the nuclear translocation and activation of NF- $\kappa$ B/p65 by inhibiting TNF- $\alpha$ -induced I $\kappa$ B $\alpha$  phosphorylation.

*Effects of PYCP on the ubiquitin-proteasome system.* To confirm that the ubiquitin-proteasome system is regulated by NF- $\kappa$ B, the protein expression levels of E3 ubiquitin ligases in C2C12 myotubes were investigated by western blot analysis. As shown in Fig. 6A, TNF- $\alpha$  treatment significantly increased atrogin-1/MAFbx and MuRF1 expression levels. However, treatment with PYCP attenuated the TNF- $\alpha$ -induced increase in the expression of atrogin-1/MAFbx and MuRF1 (Fig. 6A). In addition, to assess the protective effect of PYCP on 20S proteasome activity, the proteolytic activity of 20S proteasome was monitored by measuring the AMC fluorescence. As shown in Fig. 6B, TNF- $\alpha$  treatment significantly increased 20S proteasome activity, but this was significantly attenuated by PYCP treatment.

*Effects of PYCP on IL-6 production.* To evaluate the effect of PYCP on proinflammatory cytokines regulated by the transcription factor NF- $\kappa$ B, IL-6 production in C2C12 myotubes was measured using an ELISA kit. Increased IL-6 levels in

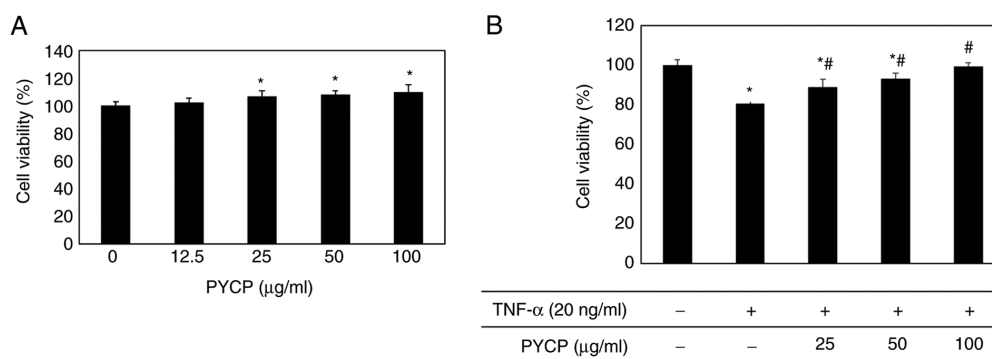


Figure 1. Effects of TNF- $\alpha$  and PYCP on the cytotoxicity of C2C12 myotubes. (A) The cell viability of C2C12 myotubes in the presence of 0, 12.5, 25, 50, and 100  $\mu\text{g/ml}$  PYCP for 24 h. (B) The cell viability of C2C12 myotubes treated with 25, 50, and 100  $\mu\text{g/ml}$  PYCP for 24 h and cotreated with 20 ng/ml TNF- $\alpha$  for 24 h. \* $P < 0.05$  vs. control untreated cells; # $P < 0.05$  vs. TNF- $\alpha$ -only treated cells. PYCP, *Pyropia yezoensis* protein; TNF- $\alpha$ , tumor necrosis factor- $\alpha$ .

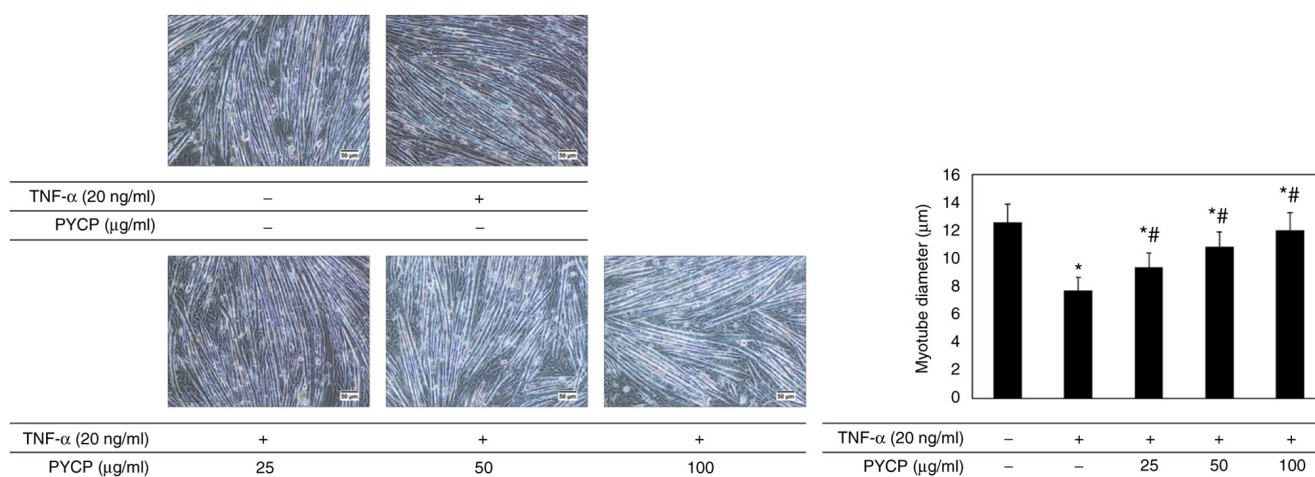


Figure 2. Effects of PYCP on myotube diameter in TNF- $\alpha$ -treated C2C12 myotubes. Representative images and quantification of myotube diameters are shown for C2C12 myotubes treated with 20 ng/ml TNF- $\alpha$  and PYCP (25, 50, or 100  $\mu\text{g/ml}$ ) for 48 h. Images were captured at  $\times 20$  magnification (scale bar, 50  $\mu\text{m}$ ). Data are presented as the mean  $\pm$  standard deviation of three independent experiments. \* $P < 0.05$  vs. untreated cells; # $P < 0.05$  vs. TNF- $\alpha$ -only treated cells. PYCP, *Pyropia yezoensis* protein; TNF- $\alpha$ , tumor necrosis factor- $\alpha$ .

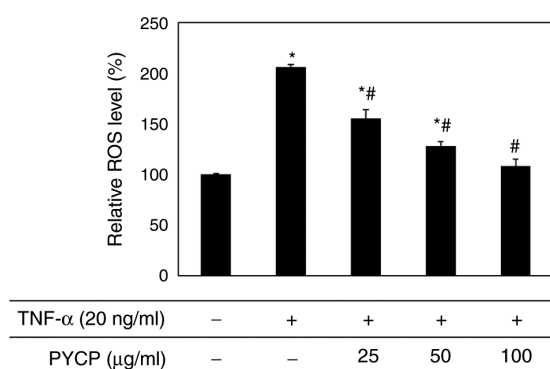


Figure 3. Effects of PYCP on the production of intracellular ROS in TNF- $\alpha$ -treated C2C12 myotubes. C2C12 myotubes were treated with 20 ng/ml TNF- $\alpha$  and PYCP (25, 50, or 100  $\mu\text{g/ml}$ ) for 48 h. Intracellular ROS production was measured using DCF-DA and fluorescence intensity analysis. Data are presented as the mean  $\pm$  standard deviation of three independent experiments. \* $P < 0.05$  vs. untreated cells; # $P < 0.05$  vs. TNF- $\alpha$ -only treated cells. PYCP, *Pyropia yezoensis* protein; ROS, reactive oxygen species; TNF- $\alpha$ , tumor necrosis factor- $\alpha$ .

TNF- $\alpha$ -treated C2C12 myotubes were significantly reduced by PYCP treatment in a dose-dependent manner (Fig. 7).

**Effects of PYCP on myogenesis.** To determine whether PYCP treatment altered myogenic differentiation in TNF- $\alpha$ -treated C2C12 myotubes, MyoD and myogenin protein expression levels were examined by western blot analysis. As shown in Fig. 8, both MyoD and myogenin protein expression levels were significantly decreased in TNF- $\alpha$ -stimulated C2C12 myotubes compared with control untreated myotubes. However, the TNF- $\alpha$ -mediated downregulation of MyoD and myogenin was significantly reversed by treatment with PYCP (Fig. 8).

## Discussion

In the present study, the antiatrophic activities and mechanisms of PYCP were investigated using TNF- $\alpha$ -treated C2C12 myotubes. The main findings demonstrated that PYCP efficiently inhibited the expression of E3 ubiquitin ligases, 20S proteasome activity, and IL-6 secretion via suppression of the NF- $\kappa\text{B}$  pathway by inhibiting TNF-R1 expression and ROS production in TNF- $\alpha$ -induced C2C12 myotubes. In addition, PYCP effectively increased MyoD and myogenin expression in TNF- $\alpha$ -induced C2C12 myotubes. The present results indicated that TNF- $\alpha$ -induced inflammation-related muscle atrophy could be attenuated by PYCP treatment.

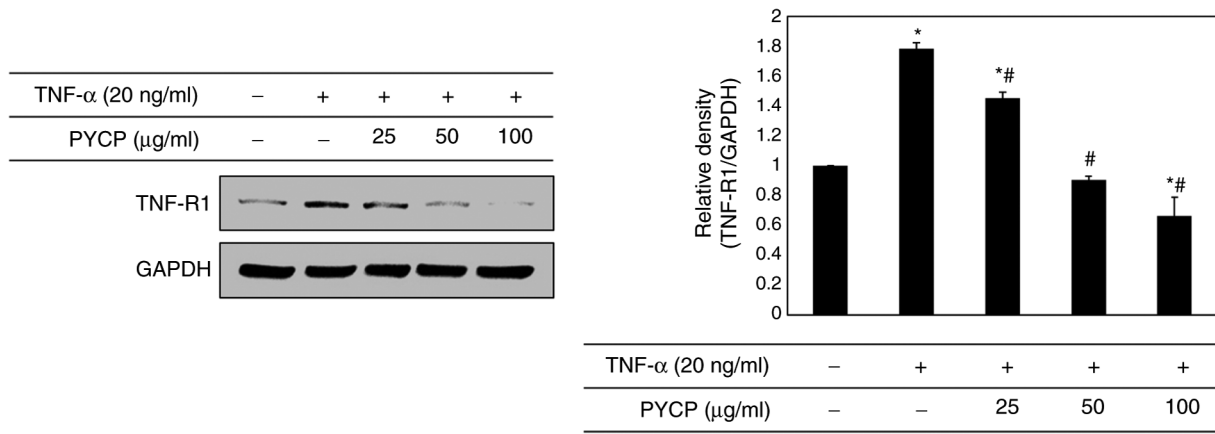


Figure 4. Effects of PYCP on the expression of TNF-R1 in TNF- $\alpha$ -treated C2C12 myotubes. TNF-R1 protein expression levels were detected by western blot analysis. GAPDH was used as an internal standard. Data are presented as the mean  $\pm$  standard deviation of three independent experiments. \* $P$ <0.05 vs. untreated cells; # $P$ <0.05 vs. TNF- $\alpha$ -only treated cells. PYCP, *Pyropia yezoensis* protein; TNF-R1, TNF receptor-1; TNF- $\alpha$ , tumor necrosis factor- $\alpha$ .

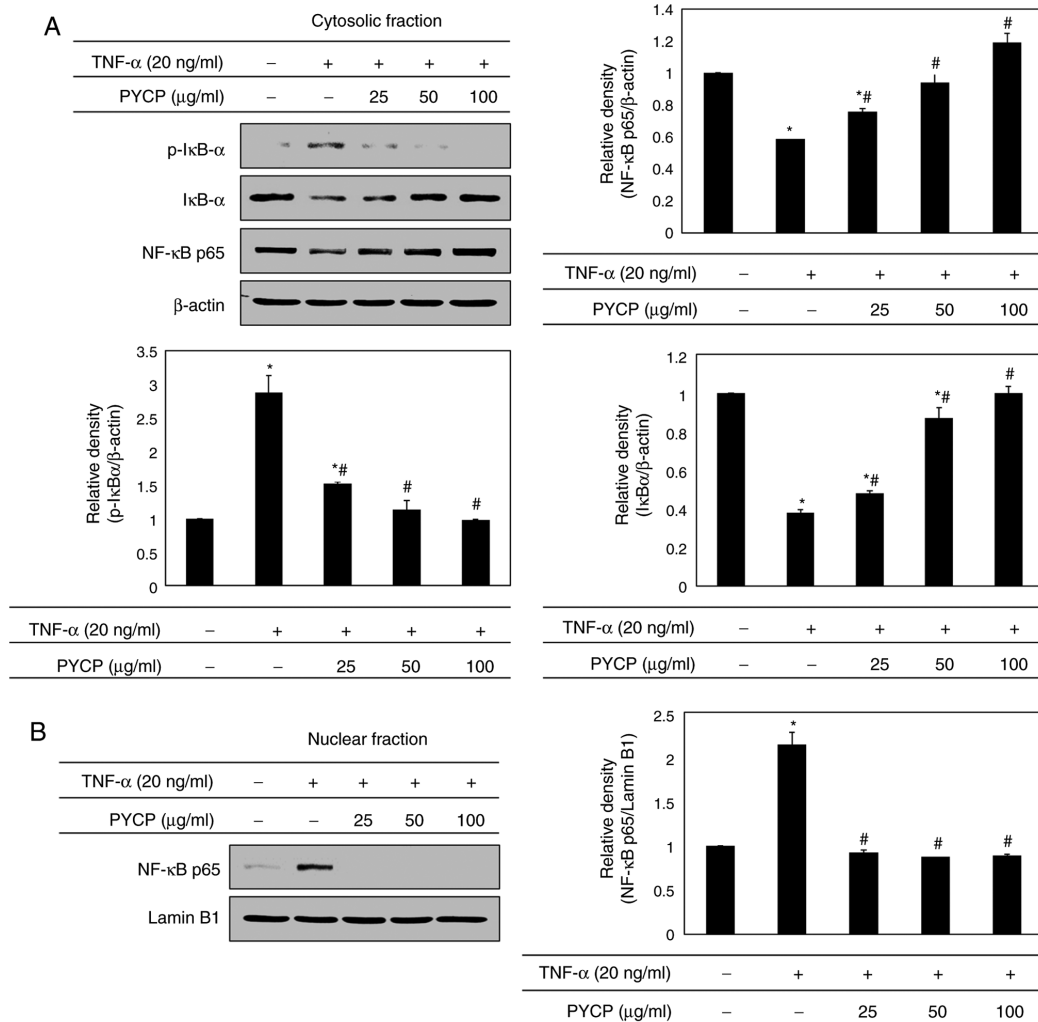


Figure 5. Effects of PYCP on the activation and translocation of NF- $\kappa$ B/p65 in TNF- $\alpha$ -treated C2C12 myotubes. (A) p-I $\kappa$ B $\alpha$ , I $\kappa$ B $\alpha$ , and NF- $\kappa$ B/p65 protein expression levels of cytosolic fractions were detected by western blot analysis. (B) NF- $\kappa$ B/p65 levels were measured in the nuclear fractions by western blot analysis.  $\beta$ -actin and lamin B1 were used as internal controls for the cytosolic and nuclear fractions, respectively. Data are presented as the mean  $\pm$  standard deviation of three independent experiments. \* $P$ <0.05 vs. untreated cells; # $P$ <0.05 vs. TNF- $\alpha$ -only treated cells. PYCP, *Pyropia yezoensis* protein; NF- $\kappa$ B, nuclear factor- $\kappa$ B; TNF- $\alpha$ , tumor necrosis factor- $\alpha$ ; p-, phosphorylated; I $\kappa$ B $\alpha$ , inhibitor of  $\kappa$ B  $\alpha$ .

'Inflammaging', the chronic low-grade inflammation that characterizes aging, is associated with muscle catabolism (26).

Additionally, an increase in body fat due to aging causes fat to be deposited in muscle tissue, and the accumulation of

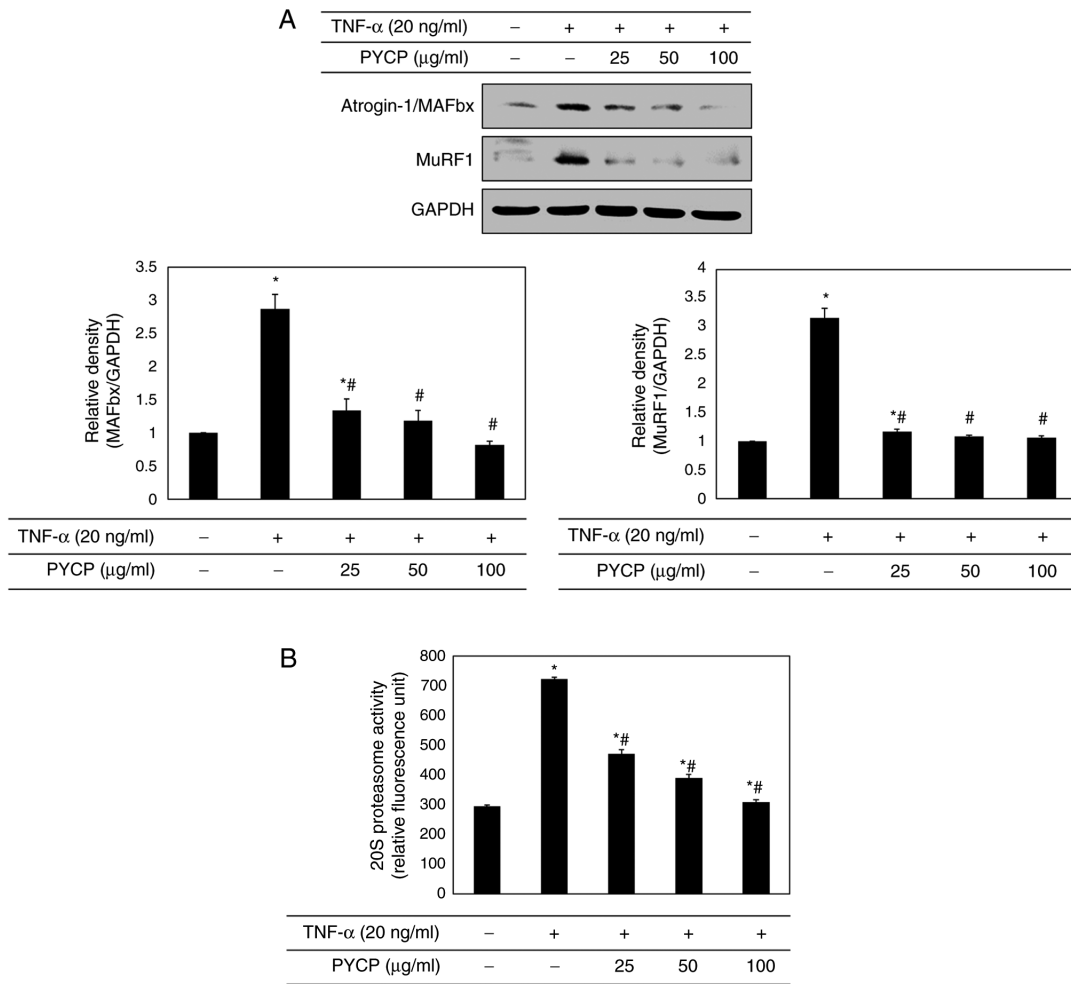


Figure 6. Effects of PYCP on the ubiquitin-proteasome system in TNF- $\alpha$ -treated C2C12 myotubes. (A) The atrogin-1/MAFbx and MuRF1 protein expression levels were detected by western blot analysis. GAPDH was used as an internal standard. (B) 20S proteasome activity was assessed by detecting AMC in cell lysates after cleavage from the AMC-tagged peptide LLVY. Data are presented as the mean  $\pm$  standard deviation of three independent experiments. \*P<0.05 vs. untreated cells; #P<0.05 vs. TNF- $\alpha$ -only treated cells. PYCP, *Pyropia yezoensis* protein; TNF- $\alpha$ , tumor necrosis factor- $\alpha$ ; MAFbx, muscle atrophy F-box; MuRF1, muscle RING-finger protein-1; AMC, 7-amino-4-methylcoumarin.

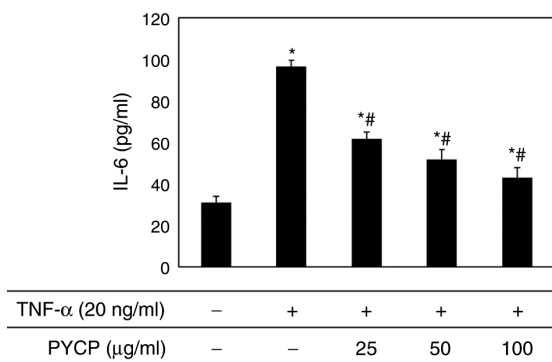


Figure 7. Effects of PYCP on the production of IL-6 in TNF- $\alpha$ -treated C2C12 myotubes. C2C12 myotubes were treated with 20 ng/ml TNF- $\alpha$  and PYCP (25, 50, or 100  $\mu$ g/ml) for 48 h. IL-6 in the culture media was measured using ELISA. Data are presented as the mean  $\pm$  standard deviation of three independent experiments. \*P<0.05 vs. untreated cells; #P<0.05 vs. TNF- $\alpha$ -only treated cells. PYCP, *Pyropia yezoensis* protein; IL-6, interleukin-6; TNF- $\alpha$ , tumor necrosis factor- $\alpha$ .

caused by the inflammatory cytokine TNF- $\alpha$  is characterized by decreases in cell survival, fiber diameter, and protein content (29,30). In the present study, TNF- $\alpha$  reduced the viability and myotube diameter of C2C12 myotubes; these effects were recovered by PYCP treatment. These results indicated that PYCP may protect C2C12 myotubes against myotube atrophy caused by TNF- $\alpha$  exposure.

The mechanisms underlying muscle atrophy are complex. The majority of the biological functions of TNF- $\alpha$  occur by TNF- $\alpha$  binding to TNF-R1 (31). Muscle atrophy caused by TNF- $\alpha$  results in loss of total muscle protein, reportedly regulated by NF- $\kappa$ B (32,33). Li *et al* showed that overexpression of I $\kappa$ B $\alpha$  sequesters NF- $\kappa$ B in an inactive state in skeletal muscle, resulting in resistance to TNF- $\alpha$ -stimulated protein degradation (34). Furthermore, the suppression of NF- $\kappa$ B activation *in vivo* improves skeletal muscle regeneration following trauma (35). Therefore, a clear association exists between TNF- $\alpha$ -induced muscle atrophy and NF- $\kappa$ B activation. In addition, the loss of muscle protein caused by NF- $\kappa$ B has been correlated with the stimulation of the ubiquitin-proteasome system and augmented by the production of intracellular ROS (36). In the present study, PYCP treatment

intramuscular fat can increase the secretion of inflammatory cytokines, such as TNF- $\alpha$  and IL-6 (27,28). Muscle atrophy

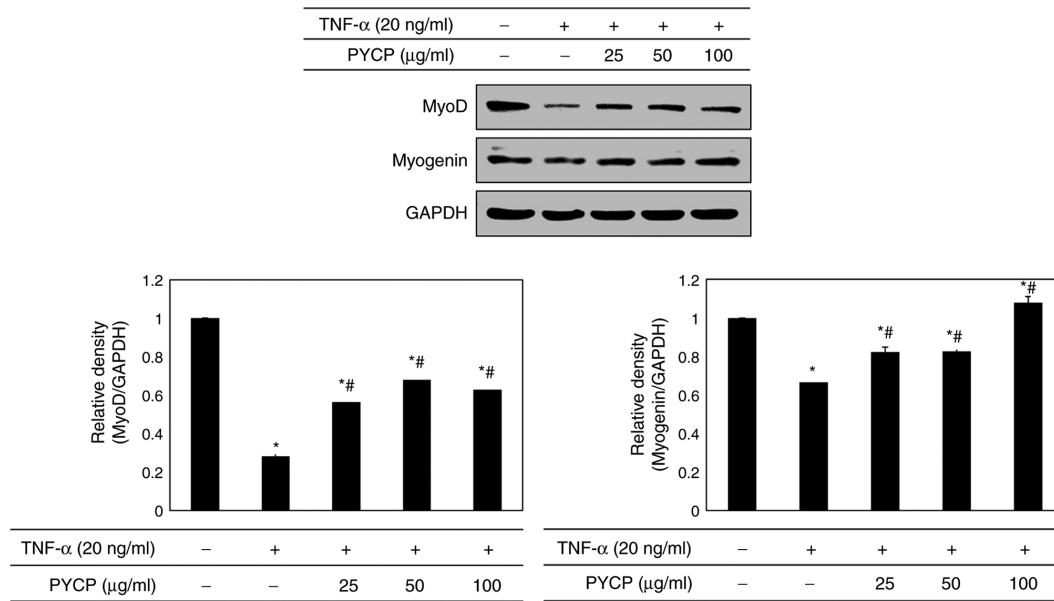


Figure 8. Effects of PYCP on the expression of MyoD and myogenin in TNF- $\alpha$ -treated C2C12 myotubes. MyoD and myogenin protein expression levels were detected by western blot analysis. GAPDH was used as an internal standard. Data are presented as the mean  $\pm$  standard deviation of three independent experiments. \*P<0.05 vs. untreated cells; #P<0.05 vs. TNF- $\alpha$ -only treated cells. PYCP, *Pyropia yezoensis* protein; MyoD, myoblast determination protein 1; TNF- $\alpha$ , tumor necrosis factor- $\alpha$ .

significantly decreased the TNF- $\alpha$ -stimulated intracellular ROS production in C2C12 myotubes, indicating that PYCP exerts antioxidant activity. Intracellular ROS contributes to the induction of E3 ubiquitin ligases by stimulating translocation of NF- $\kappa$ B to the nucleus through phosphorylation of I $\kappa$ B $\alpha$  in cultured C2C12 myotubes (36,37). In the present study, PYCP treatment inhibited the TNF- $\alpha$ -stimulated TNF-R1 expression and significantly inhibited I $\kappa$ B $\alpha$  phosphorylation and translocation of NF- $\kappa$ B to the nucleus. In addition, PYCP inhibited the expression of atrogin-1/MAFbx and MuRF1, and 20S proteasome activity stimulated by TNF- $\alpha$ . Therefore, it can be speculated that inhibition of the ubiquitin-proteasome system in the TNF- $\alpha$ -induced C2C12 myotubes was predominantly associated with the regulation of the NF- $\kappa$ B pathway through intracellular ROS removal by the antioxidant activity of PYCP.

Skeletal muscle is considered an endocrine organ capable of releasing certain cytokines and chemokines (38). The expression and release of inflammatory cytokines are promoted in TNF- $\alpha$ -treated C2C12 myotubes (39,40). Furthermore, cytokine and chemokine release from C2C12 myotubes is regulated by NF- $\kappa$ B, a transcription factor mediated by the production of free radicals, such as ROS (40). Inflammation due to the release of catabolic cytokines, such as IL-6, may contribute to muscle atrophy progression by causing muscle protein degradation (38-40). Therefore, the plasma concentration of IL-6 may be a biochemical indicator of muscle atrophy. In the present study, the TNF- $\alpha$ -stimulated production of IL-6 was reduced by PYCP treatment. Based on these results, the inhibitory effects of PYCP on the production of cytokines may be regulated by the NF- $\kappa$ B pathway through blockade of ROS production, which has a similar intrinsic antioxidant activity to PYCP. Thus, the reduction of IL-6 production from C2C12 myotubes may be primarily associated with the regulation of the NF- $\kappa$ B pathway through ROS removal due to the antioxidant activity of PYCP.

Regarding the mechanisms by which NF- $\kappa$ B influences myogenic differentiation, activation of NF- $\kappa$ B by TNF- $\alpha$  inhibits muscle differentiation through the destabilization of the MyoD and myogenin protein via a post-transcriptional mechanism (16,41). TNF- $\alpha$  and IL-1 $\beta$  have been shown to inhibit myogenic differentiation of cultured C2C12 myoblasts via activation and translocation of NF- $\kappa$ B (42). Furthermore, TWEAK, a structural homologue of TNF- $\alpha$ , can block myoblast terminal differentiation by activating NF- $\kappa$ B (43). In the present study, PYCP treatment restored the TNF- $\alpha$  reduced MyoD and myogenin expression in C2C12 myotubes. These findings are consistent with previous studies that activation of NF- $\kappa$ B by proinflammatory cytokines leads to the destabilization of MyoD and myogenin expression in skeletal muscle cells (44-46). The present data indicated that muscle atrophy progression caused by TNF- $\alpha$  may be alleviated by the PYCP-induced recovery of MyoD and myogenin expression suppressed by activation of NF- $\kappa$ B.

Overall, the present study demonstrated that the anti-atrophic effects of PYCP in TNF- $\alpha$ -stimulated C2C12 myotubes were associated with the inactivation of the NF- $\kappa$ B pathway through intracellular ROS removal by antioxidant activity. Preliminary mass spectrometry (Q-TOF MS/MS) analysis of PYCP revealed a photosystem II 12-kDa extrinsic protein (PSBU\_PYRYE, PsbU, *P. yezoensis*) (data not shown). Thus, the active ingredient of PYCP may be PsbU, an exogenous protein localized in the lumen side of photosystem II and found mostly in red algae and cyanobacteria (47). PsbU has been demonstrated to protect cells from ROS produced as an inevitable by-product of photosynthesis, by improving the thermal stability of photosystem II (48,49). Therefore, PYCP may perform the same functions as those of PsbU. Further investigations are warranted to fully elucidate the active components in PYCP and their functions and mechanisms. The results of the present study indicated that the anti-atrophic

effect of PYCP in C2C12 myotubes stimulated by TNF- $\alpha$  was associated to the inactivation of NF- $\kappa$ B through intracellular ROS removal.

### Acknowledgements

Not applicable.

### Funding

This research was supported by the Basic Science Research Program through the National Research Foundation of Korea funded by the Ministry of Education (grant nos. 2019R1A6A3A01095099 and 2012R1A6A1028677).

### Availability of data and materials

The datasets used and/or analyzed during the current study are available from the corresponding author on reasonable request.

### Authors' contributions

MKL and TJN conceived and designed the study. MKL and YHC acquired and analyzed the data. MKL and TJN confirm the authenticity of all the raw data. MKL prepared the draft of the manuscript, including the figures and table. All authors read and approved the final manuscript.

### Ethics approval and consent to participate

Not applicable.

### Patient consent for publication

Not applicable.

### Competing interests

The authors declare that they have no competing interests.

### References

- Tolosa L, Morla M, Iglesias A, Busquets X, Llado J and Olmos G: IFN-gamma prevents TNF-alpha-induced apoptosis in C2C12 myotubes through down-regulation of TNF-R2 and increased NF-kappaB activity. *Cell Signal* 17: 1333-1342, 2005.
- Lecker SH, Solomon V, Mitch WE and Goldberg AL: Muscle protein breakdown and the critical role of the ubiquitin-proteasome pathway in normal and disease states. *J Nutr* 129 (1S Suppl): 227S-237S, 1999.
- Schiaffino S, Dyar KA, Ciciliot S, Blaauw B and Sandri M: Mechanisms regulating skeletal muscle growth and atrophy. *FEBS J* 208: 4294-4314, 2013.
- Kandarian SC and Jackman RW: Intracellular signaling during skeletal muscle atrophy. *Muscle Nerve* 33: 155-165, 2006.
- Egerman MA and Glass DJ: Signaling pathways controlling skeletal muscle mass. *Crit Rev Biochem Mol Biol* 49: 59-68, 2014.
- Kirilova I, Chaisson M and Fausto N: Tumor necrosis factor induces DNA replication in hepatic cells through nuclear factor kappaB activation. *Cell Growth Differ* 10: 819-828, 1999.
- Schutze S, Machleidt T and Kronke M: Mechanisms of tumor necrosis factor action. *Semin Oncol* 19 (2 Suppl 4): S16-S24, 1992.
- Basu A, Johnson DE and Woolard MD: Potentiation of tumor necrosis factor-alpha-induced cell death by rottlerin through a cytochrome-C-dependent pathway. *Exp Cell Res* 278: 209-214, 2002.
- Li YP: TNF-alpha is a mitogen in skeletal muscle. *Am J Physiol Cell Physiol* 285: C370-C376, 2003.
- Li YP, Schwarts RJ, Waddell ID, Holloway BR and Reid MB: Skeletal muscle myocytes undergo protein loss and reactive oxygen-mediated NF-kappaB activation in response to tumor necrosis factor alpha. *FASEB J* 12: 871-880, 1998.
- Cai D, Frantz JD, Tawa NE Jr, Melendez PA, Oh BC, Lidov HG, Hasselgren PO, Frontera WR, Lee J, Glass DJ and Shoelson SE: IKKbeta/NF-kappaB activation causes severe muscle wasting in mice. *Cell* 119: 285-298, 2004.
- Mourkioti F, Kratsios P, Luedde T, Song YH, Delafontaine P, Adami R, Parente V, Bottinelli R, Pasparakis M and Rosenthal N: Targeted ablation of IKK2 improves skeletal muscle strength, maintains mass, and promotes regeneration. *J Clin Invest* 116: 2945-2954, 2006.
- Kumar A, Takada Y, Boriek AM and Aggarwal BB: Nuclear factor-kappaB: Its role in health and disease. *J Mol Med (Berl)* 82: 434-448, 2004.
- Guttridge DC, Albanese C, Reuther JY, Pestell RG and Baldwin AS Jr: NF-kappaB controls cell growth and differentiation through transcriptional regulation of cyclin D1. *Mol Cell Biol* 19: 5785-5799, 1999.
- Mitin N, Kudla AJ, Konieczny SF and Taparowsky EJ: Differential effects of Ras signaling through NFkappaB on skeletal myogenesis. *Oncogene* 20: 1276-1286, 2001.
- Berkes CA and Tapscott SJ: MyoD and the transcriptional control of myogenesis. *Semin Cell Dev Biol* 16: 585-595, 2005.
- Wang Y, Hwang JY, Park HB, Yadav D, Oda T and Jin JO: Porphyrin isolated from *Pyropia yezoensis* inhibits lipopolysaccharide-induced activation of dendritic cells in mice. *Carbohydr Polym* 229: 115457, 2020.
- Lee MK, Choi JW, Choi YH and Nam TJ: *Pyropia yezoensis* protein prevents dexamethasone-induced myotube atrophy in C2C12 myotubes. *Mar Drugs* 16: 497, 2018.
- Kim IH, Kwon MJ, Jung JH and Nam TJ: Protein extracted from porphyra yezoensis prevents cisplatin-induced nephrotoxicity by downregulating the MAPK and NF- $\kappa$ B pathways. *Int J Mol Med* 41: 511-520, 2018.
- Park SJ, Ryu J, Kim IH, Choi YH and Nam TJ: Activation of the mTOR signaling pathway in breast cancer MCF-7 cells by a peptide derived from porphyra yezoensis. *Oncol Rep* 33: 19-24, 2015.
- Choi JW, Kwon MJ, Kim IH, Kim YM, Lee MK and Nam TJ: *Pyropia yezoensis* glycoprotein promotes the M1 to M2 macrophage phenotypic switch via the STAT3 and STAT6 transcription factors. *Int J Mol Med* 38: 666-674, 2016.
- Kim CR, Kim YM, Lee MK, Kim IH, Choi YH and Nam TJ: *Pyropia yezoensis* peptide promotes collagen synthesis by activating the TGF- $\beta$ /Smad signaling pathway in the human dermal fibroblast cell line HS27. *Int J Mol Med* 39: 31-38, 2017.
- Choi JW, Kim IH, Kim YM, Lee MK, Choi YH and Nam TJ: Protective effect of *Pyropia yezoensis* glycoprotein on chronic ethanol consumption-induced hepatotoxicity in rats. *Mol Med Rep* 14: 4881-4886, 2016.
- Castillero E, Alamdari N, Lecker SH and Hasselgren PO: Suppression of atrogen-1 and MuRF1 prevents dexamethasone-induced atrophy of cultured myotubes. *Metabolism* 62: 1495-1502, 2013.
- Menconi M, Gonnella P, Petkova V, Lecker S and Hasselgren PO: Dexamethasone and corticosterone induce similar, but not identical, muscle wasting responses in cultured L6 and C2C12 myotubes. *J Cell Biochem* 105: 353-364, 2008.
- Malafarina V, Uriz-Otano F, Iniesta R and Gil-Guerrero L: Sarcopenia in the elderly: Diagnosis, physiopathology and treatment. *Maturitas* 71: 109-114, 2012.
- Kob R, Bollheimer LC, Bertsch T, Fellner C, Djukic M, Sieber CC and Fischer BE: Sarcopenic obesity: Molecular clues to a better understanding of its pathogenesis? *Biogerontology* 16: 15-29, 2015.
- Jensen GL: Inflammation: Roles in aging and sarcopenia. *JPEN J Parenter Enteral Nutr* 32: 656-659, 2008.
- Wing SS, Lecker SH and Jagoe RT: Proteolysis in illness-associated skeletal muscle atrophy: From pathways to networks. *Crit Rev Clin Lab Sci* 48: 49-70, 2011.
- Ventadour S and Attaix D: Mechanisms of skeletal muscle atrophy. *Curr Opin Rheumatol* 18: 631-635, 2006.
- Chen G and David V: TNF-R1 signaling: A beautiful pathway. *Science* 296: 1634-1635, 2002.

32. Li YP, Atkins CM, Sweatt JD and Reid MB: Mitochondria mediate tumor necrosis factor- $\alpha$ /NF- $\kappa$ B signaling in skeletal muscle myotubes. *Antioxid Redox Signal* 1: 97-104, 1999.
33. Thoma A and Lightfoot AP: NF- $\kappa$ B and inflammatory cytokine signaling: Role in skeletal muscle atrophy. *Adv Exp Med Biol* 1088: 267-279, 2018.
34. Li YP and Reid MB: NF- $\kappa$ B mediates the protein loss induced by TNF- $\alpha$  in differentiated skeletal muscle myotubes. *Am J Physiol Regul Integr Comp Physiol* 279: R1165-R1170, 2000.
35. Thaloor D, Miller KJ, Gephart J, Mitchell PO and Pavlath GK: Systemic administration of the NF- $\kappa$ B inhibitor curcumin stimulates muscle regeneration after traumatic injury. *Am J Physiol* 277: C320-C329, 1999.
36. Nisir RB, Shah DS, Ganley IG and Hundal HS: Proinflammatory NF $\kappa$ B signaling promotes mitochondrial dysfunction in skeletal muscle in response to cellular fuel overloading. *Cell Mol Life Sci* 76: 4887-4904, 2019.
37. McKinnell IW and Rudnicki MA: Molecular mechanisms of muscle atrophy. *Cell* 119: 907-910, 2004.
38. Legard GE and Pedersen BK: Muscle as an endocrine organ. *Muscle Exerc Physiol* 25: 258-307, 2019.
39. Bhatnagar S, Panguluri SK, Gupta SK, Dahiya S, Lundy RF and Kumar A: Tumor necrosis factor- $\alpha$  regulates distinct molecular pathway and gene networks in cultured skeletal muscle cells. *PLoS One* 5: e13262, 2010.
40. Lightfoot AP, Sakellariou GK, Nye GA, McArdle F, Jackson MJ, Griffiths RD and McArdle A: S $\beta$ -31 attenuates TNF- $\alpha$  induced cytokine release from C2C12 myotubes. *Redox Biol* 6: 253-259, 2015.
41. Kaliman P, Canicio J, Testar X, Palacin M and Zorzano A: Insulin-like growth factor-II, phosphatidylinositol 3-kinase, nuclear factor-kappaB and inducible nitric-oxide synthase define a common myogenic signaling pathway. *J Biol Chem* 274: 17437-17444, 1999.
42. Langen RC, Schols AM, Kelders MC, Wouters EF and Janssen-Heininger YM: Inflammatory cytokines inhibit myogenic differentiation through activation of nuclear factor-kappaB. *FASEB J* 15: 1169-1180, 2001.
43. Dogra C, Changotra H, Mohan S and Kumar A: Tumor necrosis factor-like weak inducer of apoptosis inhibits skeletal myogenesis through sustained activation of nuclear factor-kappaB and degradation of MyoD protein. *J Biol Chem* 281: 10327-10336, 2006.
44. Guttridge DC, Mayo MW, Madrid LV, Wang CY and Baldwin AS Jr: NF- $\kappa$ B-induced loss of MyoD messenger RNA: Possible role in muscle decay and cachexia. *Science* 289: 2363-2366, 2000.
45. Sitcheran R, Cogswell PC and Baldwin AS Jr: NF- $\kappa$ B mediates inhibition of mesenchymal cell differentiation through a posttranscriptional gene silencing mechanism. *Genes Dev* 17: 2368-2373, 2003.
46. Di Marco S, Mazroui R, Dallaire P, Chittur S, Tenenbaum SA, Radioch D, Marette A and Gallouzi IE: NF- $\kappa$ B-mediated MyoD decay during muscle wasting requires nitric oxide synthase mRNA stabilization, HuR protein, and nitric oxide release. *Mol Cell Biol* 25: 6533-6545, 2005.
47. Roose JL, Wegener KM and Pakrasi HB: The extrinsic proteins of photosystem II. *Photosynth Res* 92: 369-387, 2007.
48. Balint I, Bhattacharya J, Perelman A, Schatz D, Moskovitz Y, Keren N and Schwarz R: Inactivation of the extrinsic subunit of photosystem II, PsbU, in *Synechococcus* PCC 7942 results in elevated resistance to oxidative stress. *FEBS Lett* 580: 2117-2122, 2006.
49. Abasova L, Deak Z, Schwarz R and Vass I: The role of the PsbU subunit in the light sensitivity of PSII in the cyanobacterium *Synechococcus* 7942. *J Photochem Photobiol B* 105: 149-156, 2011.



This work is licensed under a Creative Commons Attribution-NonCommercial-NoDerivatives 4.0 International (CC BY-NC-ND 4.0) License.